

Direct measurement of dynamic alignment in strong fields

K. Zhao,¹ L. N. Elberson,¹ G. M. Menkir,¹ and W. T. Hill III^{1,2,*}

¹*Institute for Physical Science and Technology, University of Maryland, College Park, Maryland 20742, USA*

²*Department of Physics, University of Maryland, College Park, Maryland 20742, USA*

(Received 26 May 2006; published 19 September 2006)

The degree of dynamic alignment (the excess alignment beyond that due to geometric alignment) induced by linearly polarized, 100 fs pulses in the 10^{15} W/cm² intensity range, has been investigated. Exploiting circular polarization to turn off dynamic alignment and 4π angular collection to capture all ejected ions, a quantitative measure of the excess alignment was extracted from the relative atomic ion yields subsequent to Coulomb explosion in linearly and circularly polarized fields for several linear molecules (H₂, N₂, O₂, and CO₂). The degree of dynamic alignment was measured to be about 0.90 (H₂), 0.16 (N₂ and O₂), and 0.29 (CO₂). The anomalously large value of CO₂ implies a torque enhancement that we show is consistent with CO₂ interacting with the field longer than N₂ and O₂ prior to enhanced ionization.

DOI: [10.1103/PhysRevA.74.033408](https://doi.org/10.1103/PhysRevA.74.033408)

PACS number(s): 42.50.Hz, 33.80.-b, 42.50.Vk

The anisotropy in the angular distribution of ejected ions induced via strong-field Coulomb explosion (CE) of diatomic and polyatomic molecules following enhanced ionization (EI) has been the subject of debate for nearly two decades [1,2]. Two effects contribute to the anisotropy, the so-called geometric [1,3,4] and dynamic [4–6] alignment (GA and DA, respectively). Alignment due to GA relies on terms of the form $\langle \mathbf{p} \cdot \mathbf{E} \rangle^m$, due the multiphoton transitions (where m , in this context, is twice the number of photons involved in the transition), leading to ionization prior to EI, where \mathbf{p} ($\equiv \boldsymbol{\alpha} \cdot \mathbf{E}$) is the induced dipole moment, \mathbf{E} the electric field of the laser, and $\boldsymbol{\alpha}$ the polarizability matrix, with $\boldsymbol{\alpha}_{\parallel}$ and $\boldsymbol{\alpha}_{\perp}$ components relative to the molecular axis, \mathbf{M} . The field exerting a torque on \mathbf{M} distinguishes DA from GA. This torque induces \mathbf{M} to align with \mathbf{E} prior to EI. Tong *et al.* [7] refer to torquing the neutrals as DA and torquing the molecular ions as postionization alignment. In this paper we will use DA to refer to both processes because contributions to the angular distribution of the ejected atomic ions due to DA (torquing) can be eliminated, but we cannot determine when, before the explosion, the torque occurs.

At low intensities and with sub-10-fs pulses, the valence structure plays an important role [8]. At high intensities, however, particularly with pulses as long as 100 fs, charge-resonance transitions dominate the electron dynamics prior to CE [9]. The induced dipole is then due to moving charge from one side of the molecule to the other, which is largest when $\mathbf{p} \parallel \mathbf{M}$. As a result, $|\mathbf{p}| \propto R$, the bond length. We also can model alignment in terms of $\boldsymbol{\alpha}$, if field-induced quantities are used. However, calculations show that $|\boldsymbol{\alpha}_{\parallel}| \propto R$ while $|\boldsymbol{\alpha}_{\perp}|$ is nearly independent of R [7]. Thus, at high intensities ($\sim 10^{15}$ W/cm²), molecules with \mathbf{M} aligned more with \mathbf{E} are easier to ionize, and the ejections tend to be along \mathbf{E} and depend on $\langle \mathbf{M} \cdot \mathbf{E} \rangle^m$, even for short (< 30 fs) pulses, as addressed in Ref. [8], leading to a $\cos^m \theta$ angular distribution where θ is the angle between \mathbf{E} and \mathbf{p} (\mathbf{M}).

Typical Coulomb explosion experiments employ linearly polarized light; GA and DA are then comingled and difficult

to distinguish. Several authors have pointed out that EI will ensue without, or at least significantly reduced, DA in circularly polarized fields since the polarization axis rotates too quickly (a period of $2\pi/\omega$) for the molecule to respond to the instantaneous torque [10–13]. Thus far, previous studies have been qualitative, providing tests for determining when DA is active. These tests include varying the polarization [10–13], wavelength, and pulse width of the field [14], laser intensity [13,14], the moment of inertia [10], and the charge state of the constituent atoms [10,12–14], as well as comparing two-dimensional over-the-barrier ionization calculation with anisotropy measurement [3]. In general, DA increases as the moment of inertia decreases and the laser intensity increases. While it appears to be clear that DA is inactive in I₂ [3,10] and active in H₂ [3], N₂ [3,11,13,14], O₂ [10], and CO₂ [11,12], a quantitative measure of the contribution each type of alignment makes to the anisotropy has never been reported, to our knowledge. The purpose of this paper is to fill this void for four linear systems, H₂, N₂, O₂, and CO₂. To that end, we compare explosion spectra induced by linearly and circularly polarized fields, while exploiting our ability to image (collect) all explosion ejecta simultaneously. This approach not only distinguishes the two effects, it provides a quantitative measure of the contribution DA makes to the anisotropy.

Our characterization of DA is based on the relative number of atomic ions,

$$n = \frac{N_{LP}}{N_{CP}}, \quad (1)$$

measured under linearly (N_{LP}) and circularly (N_{CP}) polarized fields. In the absence of DA, $N_{LP} < N_{CP}$ and $n \rightarrow n_G$, where the subscript G indicates the population ionizes solely through GA. As mentioned above, the number of ions generated via GA depends on m and can be written as

*Electronic address: wth@ipst.umd.edu

$$\begin{aligned}
n_G(m) &= \frac{N_{LP_G}}{N_{CP_G}} = \frac{2 \int_0^{2\pi} \int_0^{\pi/2} \cos^m \theta d\Omega}{2 \int_0^{2\pi} \int_0^{\pi/2} \cos^m(\pi/2 - \theta) d\Omega} \\
&= \frac{2}{\sqrt{\pi}(1+m)} \frac{\Gamma\left(\frac{3+m}{2}\right)}{\Gamma\left(\frac{2+m}{2}\right)}, \quad (2)
\end{aligned}$$

where $d\Omega$ is the solid angle and the distribution of molecules is assumed to be isotropic. The origin of this expression can be understood as follows. First we note that at 10^{15} W/cm², all molecules aligned with \mathbf{E} ($\theta=0$) are ionized [15]. Thus, when N_0 molecules are in the laser focus, N_{LP_G} will be given by $N_0/(1+m)$ (i.e., in the absence of DA). Only those ions within a relatively small cone angle about \mathbf{E} are ionized. At the same time, N_{CP_G} is given by $(\sqrt{\pi}N_0/2)\Gamma((2+m)/2)/\Gamma((3+m)/2)$. The z axis for the N_{CP_G} integral is perpendicular to the plane of polarization, to account for the fact that molecules within a wedge angle measured from this plane are ionized. Many more, but not necessarily all, molecules are ionized in circularly polarized fields (e.g., $N_{LP_G} \approx 0.08N_0$, while $N_{CP_G} \approx 0.34N_0$ at $m=12$) due to the different integration regions. As a measure of DA, we define a dimensionless parameter we call the degree of dynamic alignment,

$$\eta = \frac{n - n_G}{1 - n_G}, \quad (3)$$

which ranges from 0 (no DA) to 1. Clearly, this reflects the fact that in the absence of DA $n \rightarrow n_G$ and when all molecules are aligned with \mathbf{E} (complete DA), $N_{LP} \rightarrow N_{CP} \rightarrow N_0$ and $n \rightarrow 1$. If we define the number of molecules responding to DA as $N_0\Delta n_{LP} = N_{LP} - N_{LP_G}$ and $N_0\Delta n_{CP} = N_{CP} - N_{CP_G}$, respectively, for linearly and circularly polarized fields, an explicit expression relating Δn_{LP} and Δn_{CP} to η can be derived from Eqs. (1)–(3),

$$\Delta n_{LP} - n\Delta n_{CP} = \eta(1 - n_G) \frac{N_{CP_G}}{N_0} = \eta(1 - n_G) \frac{\pi}{2} \frac{\Gamma\left(\frac{2+m}{2}\right)}{\Gamma\left(\frac{3+m}{2}\right)}. \quad (4)$$

Consequently, η is sufficient to characterize DA.

To measure N_{LP} and N_{CP} , we employed an experimental arrangement similar to that in Ref. [21], where the explosion partners with momenta parallel to the face of the detector up to $\sim 80\sqrt{qM}$ a. u., where qe is the charge and M is the atomic mass, were captured simultaneously with our 4π -image spectrometer [21,22] subsequent to excitation of the parent molecule with linearly or near circularly polarized, 800 nm radiation. Focused 100 fs pulses could be varied in intensity from 0.5 to 5×10^{15} W/cm² without modifying other parameters. The spectrometer consists of a uniform extraction field and image quality microchannel plates (MCP) backed by a

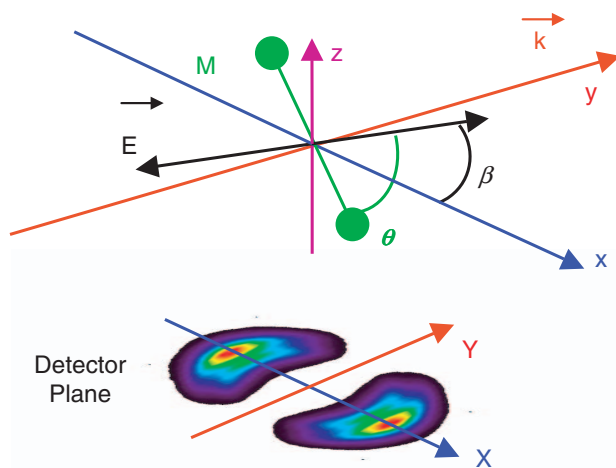


FIG. 1. (Color online) Coordinates in the focal and detector planes, separated by a distance l , with the x (y) axis parallel to the X (Y) axis. The laser is polarized in the xz plane at an angle β and the molecular axis (M) is oriented at an angle θ relative to \mathbf{E} .

phosphor screen and housed in a vacuum chamber. Sample gas pressures were in the 0.1 and 6×10^{-8} Torr range. Images were recorded at 500 Hz with a digital CCD camera synchronized to the laser repetition rate—each image frame corresponded to one laser pulse and contained only a few explosion events (0 to ~ 10). Knowing that ions with different charge-to-mass ratios arrive at the detector at different times, we gated the potential across the MCP to select the ions of interest to record. Gate widths of a few hundred nanoseconds are sufficient to isolate the first few charge states of atomic ions. Values for N_{LP} and N_{CP} were obtained by integrating the total charge signal associated with an image. In these experiments, each image contained 200 000 laser shots.

Linearly polarized radiation was generated directly from a Ti:Sapphire regenerative amplifier. Elliptical polarization was generated with a $\lambda/4$ plate. Our experiments were run with an ellipticity, ϵ , of about 0.92, where $\epsilon = E^</math>/ $E^>$. The electric field along the major (minor) axis is indicated by the superscript $>$ ($<$); $E^<=0$ corresponds to linear polarization. The direction of the major axis was controlled with a $\lambda/2$ plate. We assume EI occurs at the critical radius, R_C [9], which is determined by the field strength. Thus, to keep the field the same, the circular polarization intensity was twice that of the linear polarization. When $\epsilon=0.92$, the electric fields are nearly the same for elliptically (EP) and linearly (LP) polarized fields— $E_{EP}^> \approx 1.04E_{LP}$ and $E_{EP}^< \approx 0.96E_{LP}$. To approximate circular polarization more closely, we averaged four images with $E_{EP}^>$, confined to the xz plane (see Fig. 1), pointing in two orthogonal directions by rotating the $\lambda/2$ plate through 180° .$

We extract n from Fig. 2 where we present the results of three separate explosion experiments performed with linear polarization with \mathbf{E} along $\hat{\mathbf{x}}$ (see Fig. 1), circular polarization with \mathbf{E} in the xz plane and linear polarization with \mathbf{E} confined to the xz plane and β rotated through π rad. Since the physics is independent of β , N_{LP} should be approximately

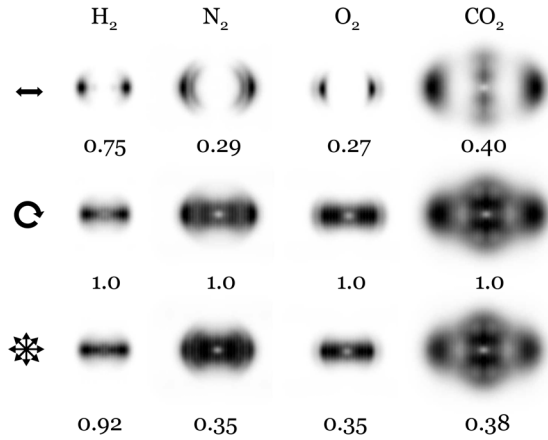


FIG. 2. Momentum distributions for linear explosions at $I_0=2 \times 10^{15}$ W/cm² and $\beta=0^\circ$ (top), circular explosions at $2I_0$ (middle), and linear explosions at I_0 averaged over 18 angles for β ranging from 0° to 170° in steps of 10° (bottom) along with the relative yields. The N₂ and O₂ images contain doubly charged ions, CO₂ images contain doubly and triply charged ions while H₂ images contain protons exclusively.

the same for top and bottom rows. This is clearly not the case, which is due primarily to gain variation over the MCP. A better estimate of N_{LP} is given by the bottom row. We emphasize that the bottom row is an average, not a sum, of 18 separate experiments so the number of counts measured corresponds to a single linear polarization experiment. At the same time, charges are collected over the same area of the plate in the middle and bottom rows. The first point explains why when DA is incomplete, the bottom row has a lower yield than the middle row—the denominator of Eq. (2) is larger than the numerator. The second point ensures that gain variation across the plate is the same in the two cases. Consequently, n is given by the relative yields of the bottom row.

Figure 3 displays n vs m for the four systems along with an estimate of η , which graphically is related to the relative distance to the upper and lower curves. Clearly, η is sensitive to m . The values plotted correspond to m_{avg} , a weighted average of the dominant channels for each system as discussed in the next paragraph. We determined m for specific channels from fits to angular distributions measured from correlated explosion partners as described in Ref. [23]. While at a given intensity m is independent of bond angle for CO₂, it is affected by several other parameters for all the systems. First,

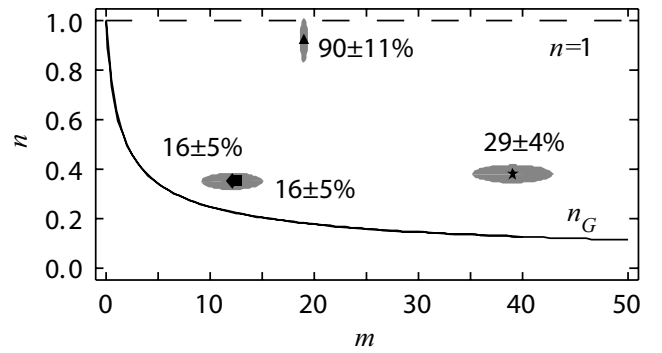


FIG. 3. Relative ion yield, n vs m , for H₂ (triangle, 0.92 ± 0.09), N₂ (diamond, 0.35 ± 0.04), O₂ (square, 0.35 ± 0.04), and CO₂ (star, 0.38 ± 0.04). The grey ranges, centered at n and m_{avg} (see text), indicate the uncertainties in our determination. The solid (dashed) curve is n_G ($n=1$) and the η values for each point are given as percentages adjacent to each point.

it depends on the intensity. At high enough intensities, ionization will saturate and all molecules within a cone angle α relative to \mathbf{E} will ionize; α grows with intensity, broadening the distribution and reducing the apparent m . To explore this behavior, we varied the intensity between 1 and 4×10^{15} W/cm² and found m to be constant within 7%. Wider intensity excursions caused m to exhibit larger variations. This is due in part to opening and closing of different ionization channels; m increases monotonically with ionization stage [13,14].

Since the images in Fig. 2 are composed of several channels, except for H₂, m and η will be between the values for the dominant channels listed in Table I. The table also contains the corresponding measured m and contribution this channel makes to the images in Fig. 2, m_{avg} for each system and an average full width, $\Delta\theta_{avg}$, associated with m_{avg} . We note that m_{avg} is only approximate for CO₂ because the correlation signals between the doubly and triply charged ions were too weak to determine the angular distributions for mixed charge-state channels. The fact that m increases with the charge state means m_{avg} should be considered a lower limit for CO₂. Since $n_G(m)$ has a negative slope, η for CO₂ is also a lower limit. Since n_G is very flat near $m=40$, η is not very sensitive to the actual value of m in this region, as can be seen in Fig. 3. The grey areas about the data points in Fig. 3 is an estimate of the uncertainty in n and m . The primary uncertainty in n is due to variations in N_{LP} and N_{CP} , which was about 7%. The uncertainty in m is due mostly to the

TABLE I. Parameters for DA for 100 fs, 800 nm pulses at 2×10^{15} W/cm²: primary and secondary channels along with $[m]$ and (%) contribution), R_e and R_C in nm, $\Delta\theta_{avg}$ ($\Delta\theta_{da}$) the average (apparent) full width of the angular distribution for m_{avg} (m_{da}), η , n , Δn , and $T_i/T_i(O_2)$ calculated at $\langle R_{mol} \rangle = (R_e + R_C)/2$ as discussed in the text.

	Primary channel	Secondary channel	R_e	R_C	m_{avg}	$\Delta\theta_{avg}$	m_{da}	$\Delta\theta_{da}$	η	n	Δn	$T_i/T_i(O_2)$
H ₂	1,1 [19] (100%)	none	0.074	0.25	19.0	31°	0.13	179.4°	90±11%	0.92	0.74	1.4, 17
N ₂	2,2 [15] (62%)	2,1 [7] (38%)	0.110	0.23	12.1	38.6°	4.67	60.9°	16±5%	0.35	0.12	0.8, 0.9
O ₂	2,1 [11] (62%)	2,2 [15] (38%)	0.121	0.23	12.5	37.8°	4.67	60.9°	16±5%	0.35	0.13	1, 1
CO ₂	2,2,2 [39] (80%)	2,3,2/3,2,3/3,2,2 [-] (20%)	0.232	0.44	~39	22°	3.88	66.5°	29±4%	0.38	0.25	2.7, 2.4

multiple channels mentioned above. This explains the large horizontal uncertainty for all systems but H₂, which only has one channel. For CO₂, we took the uncertainty in m to be $\sim 10\%$. Again, η is not very sensitive to m near $m=40$. The contribution due to the uncertainty in extracting m from fits to the angular distributions is much less than 10% and negligible except for H₂. The corresponding uncertainty in the values for η are given in both Fig. 3 and Table I.

The first conclusion we draw from Fig. 3 and Table I is that DA is essentially the same for N₂ and O₂. This is consistent with the fact that the R_C s, the charge states and the moments of inertia are all about the same. The second is that H₂ is torqued more efficiently than the other systems. This is not surprising since H₂ has a significantly smaller moment of inertia, which causes its free rotation to be faster as well as making it easier to be torqued. A third conclusion is η for CO₂ ranks second behind H₂. This is surprising. While the induced dipole moment sustained by charge-resonance states ($|\mathbf{p}| \propto eR_{mol}$ [9], where R_{mol} is the total length of the molecule) increases relative to N₂ and O₂, the moment of inertia of CO₂ is larger ($I_M \propto R_{mol}^2/4$), making it more difficult for CO₂ to respond to the same torque at both R_e (the equilibrium separation) and R_C (Table I). At the same time, a higher ionization stage of the molecule is consistent with the precursor ion spending more time in the field [13,14]—H₂²⁺, N₂⁴⁺, O₂⁴⁺, and CO₂⁶⁺. Evidently, a longer interaction time with the field, perhaps combined with multiphoton ionization prior to EI, leads to a significant enhancement in the number of molecules torqued beyond that expected from the ratio $|\mathbf{p} \times \mathbf{E}|/I_M$, which governs the classical equation of motion for θ . We point out that a larger perpendicular component of \mathbf{p} (or \mathbf{a}_\perp) that will arise when CO₂ is bent does not solve this mystery as it will tend to retard DA making the problem worse.

The exact nature of the enhancement requires more knowledge of the evolution of the systems in the field than we have. However, we can show that it is consistent with a longer interaction time with the field, T_i . In the simplest model the population torqued $\propto T_i$. However, since we only know n and not N_{LP}/N_0 and N_{CP}/N_0 (which depends on knowledge of quantum efficiency, etc.) required to determine Δn_{LP} and Δn_{CP} , we will use $\Delta n = n - n_G$ as a measure of the population torqued. The relative interaction time can be written as $T_i(\text{CO}_2)/T_i(\text{O}_2) \propto \Delta n(\text{CO}_2)/\Delta n(\text{O}_2)$ because molecules nearly aligned with \mathbf{E} will be trapped in pendular states at 10^{15} W/cm² [23,24]. The proportionality coefficient depends on the moments of inertia and molecular lengths of the two systems, which we determine from the equation of motion, $\ddot{\theta} = -(pE \sin \theta)/I_M$. We ignored the damping term, $(2\dot{R}\dot{\theta}/R)$, because it has been shown to be small at 10^{15} W/cm² [10,25]. Since the dipole is established by the field, $p \propto eR \cos \theta$, this leads to

$$\ddot{\theta} = -\frac{E \sin \theta \cos \theta}{a^2 MR}, \quad (5)$$

where a depends on how p is related to R , which is nearly independent of variations in R and θ . Assuming the molecules start from rest at angle θ , integrating the $\ddot{\theta}$ equation

shows it takes time $T(\theta) = aK(\sin^2 \theta)\sqrt{MR/E}$ for the system to rotate to 0, where $K(\sin^2 \theta)$ is the elliptic integral of the first kind. At the same time, numerical models show that $p \approx 0.5R$ for H₂⁺ [9] and $0.4R$ for H₃²⁺ [26]. Thus, a is nearly the same for diatomics (H₂⁺) and triatomics (H₃²⁺). Assuming this holds for N₂, O₂, and CO₂ (we are aware of no calculations to the contrary) the proportionality coefficient is just $\sqrt{R(\text{CO}_2)/R(\text{O}_2)}$ allowing the relative interaction to be written as

$$\frac{T_i(\text{CO}_2)}{T_i(\text{O}_2)} = \frac{\Delta n(\text{CO}_2)}{\Delta n(\text{O}_2)} \sqrt{\frac{R(\text{CO}_2)}{R(\text{O}_2)}}. \quad (6)$$

Values for the relative times are given as the first number under the last column in Table I. Since we do not know where the systems are torqued most efficiently, we chose an average R between R_e and R_C for this comparison. The result is CO₂ spends about 2.7 times longer in the field than O₂. While T_i is about the same for O₂ and N₂, this model suggests H₂ spends about 40% more time in the field than O₂. We point out that these ratios depend on the values selected for R . If, for example, H₂ were torqued more efficiently near its R_e , while O₂ closer to its R_C , this model would suggest H₂ spends 20% less time than O₂. Since H₂ loses only two electrons while the others lose more, it is very possible that H₂ receive more torque closer to R_e than the others.

It is also possible to estimate T_i directly from $T(\theta)$ if we recognize that the population torqued for a specific m_{avg} lie outside $\Delta\theta_{avg}$, the width of the angular distribution given in Table I. In the absence of DA, only the molecules within this cone, n_G , will be ionized. For n to exceed n_G , additional molecules must be rotated into this cone prior to EI. Since $K(\sin^2 \theta)$ increases monotonically with θ from 0 to 90°, it becomes harder and harder to rotate molecules as θ increases. We can estimate the width of the distribution of the molecules responding to DA, $\Delta\theta_{da}$, from an apparent exponent, m_{da} , which we obtain by equating $n_G(m_{da})$ with the measured n . The interaction time can be estimated by calculating ΔT for rotating from θ_{da} ($=\Delta\theta_{da}/2$) to θ_{avg} ($=\Delta\theta_{avg}/2$)— $T_i = T(\theta_{da}) - T(\theta_{avg})$. The relative interaction times in this approach are given as the second number in the last column in Table I. Except for H₂, we have good agreement between the two methods. Again, the time for H₂ is most likely too large not only because of uncertainty in the molecular lengths but because we have assumed that the molecules are not rotating. A combination of the facts that $K(\sin^2 \theta) \rightarrow \infty$ as $\theta \rightarrow 90^\circ$ and that $\theta_{da} \lesssim 90^\circ$, explains why the time for H₂ is so long. Since H₂ rotates rather rapidly compared with the other systems, it is not necessary for the field to do all the work; most H₂ will rotate to much smaller angles. For example, if $\theta_{da} = 59^\circ$, $R_{H_2} = R_e$ and $R_{O_2} = R_C$, the rotation times for H₂ and O₂ would be about the same.

In conclusion, we have reported a general technique for measuring the contribution geometric and dynamic alignment make to the ejection anisotropy. Our measurements not only confirmed previous qualitative observations, they provided a quantitative measure of the degree of DA. We also show that the anomalously large DA in the linear triatomic, CO₂, is consistent with the removal of more electrons prior

to the Coulomb explosion, thus the precursor ion spends more time in the field than diatomic systems such as N_2 and O_2 . While our simple classical model sheds some light on the underlying physics, a full quantum mechanical treatment is necessary to confirm these ideas and the interaction times. At the same time, the potential contribution that angular

momentum introduced by circular polarization [27] makes to the anisotropy needs to be investigated.

We thank V. Chintawar, Ph. Land (REU Student), and M. Laich (REU Student) for technical assistance. This work was supported by the National Science Foundation Grant No. PHY0245592.

-
- [1] L. J. Frasinski, K. Codling, P. Hatherly, J. Barr, I. N. Ross, and W. T. Toner, *Phys. Rev. Lett.* **58**, 2424 (1987).
- [2] C. Cornaggia, *Phys. Rev. A* **54**, R2555 (1996).
- [3] J. H. Posthumus, J. Plumridge, M. K. Thomas, K. Codling, L. J. Frasinski, A. J. Langley, and P. F. Taday, *J. Phys. B* **31**, L553 (1998).
- [4] H. Stapelfeldt and T. Seideman, *Rev. Mod. Phys.* **75**, 543 (2003).
- [5] D. Normand, L. A. Lompré, and C. Cornaggia, *J. Phys. B* **25**, L497 (1992).
- [6] P. Dietrich, D. T. Strickland, and P. B. Corkum, *J. Phys. B* **26**, 2323 (1993).
- [7] X. M. Tong, Z. X. Zhao, A. S. Alnaser, S. Voss, C. L. Cocke, and C. D. Lin, *J. Phys. B* **38**, 333 (2005).
- [8] A. S. Alnaser, C. M. Maharjan, X. M. Tong, B. Ulrich, P. Ranitovic, B. Shan, Z. Chang, C. D. Lin, C. L. Cocke, and I. V. Litvinyuk, *Phys. Rev. A* **71**, 031403(R) (2005).
- [9] S. Chelkowski and A. D. Bandrauk, *J. Phys. B* **28**, L723 (1995).
- [10] C. Ellert and P. B. Corkum, *Phys. Rev. A* **59**, R3170 (1999).
- [11] P. Hering and C. Cornaggia, *Phys. Rev. A* **59**, 2836 (1999).
- [12] W. A. Bryan, J. H. Sanderson, A. El-Zein, W. R. Newell, P. Taday, and A. J. Langley, *J. Phys. B* **33**, 745 (2000).
- [13] K. Miyazaki, T. Shimizu, and D. Normand, *J. Phys. B* **37**, 753 (2004).
- [14] M. Schmidt, S. Dobosz, P. Meynadier, P. D'Oliveira, D. Normand, E. Charron, and A. Suzor-Weiner, *Phys. Rev. A* **60**, 4706 (1999).
- [15] The ionization signal for neutral atoms [16,17] and molecules [18] is observed to saturate below 10^{15} W/cm² at low frequencies, indicating a zero survival probability in the focus. Theoretical predictions via over-the-barrier ionization models agree [16,19,20].
- [16] S. Augst, D. Strickland, D. D. Meyerhofer, S. L. Chin, and J. H. Eberly, *Phys. Rev. Lett.* **63**, 2212 (1989).
- [17] S. Augst, A. Talebpour, S. L. Chin, Y. Beaudoin, and M. Chaker, *Phys. Rev. A* **52**, R917 (1995).
- [18] C. Cornaggia and P. Hering, *Phys. Rev. A* **62**, 023403 (2000).
- [19] A. D. Bandrauk, S. Chelkowski, T. Zuo, and H. Yu, in *AIP Conference Proceedings, Resonance Ionization Spectroscopy 1996: Eighth International Symposium*, edited by N. Winograd and J. E. Parks (AIP, New York, 1997), Vol. 388, p. 37.
- [20] A. D. Bandrauk and J. Ruel, *Phys. Rev. A* **59**, 2153 (1999).
- [21] K. Zhao, T. Colvin, Jr., W. T. Hill, III, and G. Zhang, *Rev. Sci. Instrum.* **73**, 3044 (2002).
- [22] J. Zhu and W. T. Hill, III, *J. Opt. Soc. Am. B* **14**, 2212 (1997).
- [23] K. Zhao and W. T. Hill, III, *Phys. Rev. A* **71**, 013412 (2005).
- [24] B. Friedrich and D. Herschbach, *Phys. Rev. Lett.* **74**, 4623 (1995).
- [25] S. Banerjee, D. Mathur, and G. R. Kumar, *Phys. Rev. A* **63**, 045401 (2001).
- [26] H. Yu and A. D. Bandrauk, *Phys. Rev. A* **56**, 685 (1997).
- [27] S. Banerjee, G. R. Kumar, and D. Mathur, *Phys. Rev. A* **60**, R25 (1999).